Research Article

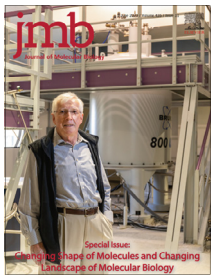


# Insights into the Structure of Invisible Conformations of Large Methyl Group Labeled Molecular Machines from High Pressure NMR

**Christina Krempl, Jan Philip Wurm, Markus Beck Erlach, Werner Kremer and Remco Sprangers** *

***Institute of Biophysics and Physical Biochemistry,*** *Regensburg Center for Biochemistry, University of Regensburg, 93053 Regensburg, Germany*

***Correspondence to Remco Sprangers:*** *remco.sprangers@ur.de (R. Sprangers)*
https://doi.org/10.1016/j.jmb.2022.167922
***Edited by M.F. Summers***

## Abstract

Most proteins are highly flexible and can adopt conformations that deviate from the energetically most favorable ground state. Structural information on these lowly populated, alternative conformations is often lacking, despite the functional importance of these states. Here, we study the pathway by which the Dcp1:Dcp2 mRNA decapping complex exchanges between an autoinhibited closed and an open conformation. We make use of methyl Carr–Purcell–Meiboom–Gill (CPMG) NMR relaxation dispersion (RD) experiments that report on the population of the sparsely populated open conformation as well as on the exchange rate between the two conformations. To obtain volumetric information on the open conformation as well as on the transition state structure we made use of RD measurements at elevated pressures. We found that the open Dcp1:Dcp2 conformation has a lower molecular volume than the closed conformation and that the transition state is close in volume to the closed state. In the presence of ATP the volume change upon opening of the complex increases and the volume of the transition state lies in-between the volumes of the closed and open state. These findings show that ATP has an effect on the volume changes that are associated with the opening-closing pathway of the complex. Our results highlight the strength of pressure dependent NMR methods to obtain insights into structural features of protein conformations that are not directly observable. As our work makes use of methyl groups as NMR probes we conclude that the applied methodology is also applicable to high molecular weight complexes.



## Introduction

Proteins are highly dynamic biomolecules that can sample different structural states. Many of these conformations are functionally relevant, especially in enzymes that need to change conformation to interact with substrates, to form a catalytically competent state or to release the reaction products. For many proteins our current structural knowledge is, however, limited to a static image of one of the possible states that a biomolecule can adopt.[1] This visualized state is, however, not necessarily occupied to the largest degree in solution, or catalytically important. Solution state NMR spectroscopy is especially suited to study conformational changes and to determine the associated thermodynamic and kinetic parameters. These data can then complement static structural information, such that a more complete picture of the protein energy landscape can be obtained.[2–6]

In the following, we consider a protein that dynamically exchanges between two structurally different states A and B (with the forward rate $k_{AB}$ and the backward rate $k_{BA}$, where

$k_{ex} = k_{AB} + k_{BA}$): $A \underset{k_{BA}}{\overset{k_{AB}}{\rightleftarrows}} B$. The populations of A ($p_A$) and B ($p_B = 1 - p_A$) and the equilibrium constant $K_{eq} = p_B/p_A$ are determined by the (Gibbs) free energy difference $\Delta G_{AB}$ between the two states according to: $\Delta G_{AB} = G_B - G_A = -RTln(K_{eq})$, where $R$ is the gas constant and $T$ is the absolute temperature. The free energy difference between A and B can be modulated by several means, including changes in the sample conditions (pH, salt or the addition of denaturants) or by changing other experimental parameters (temperature or hydrostatic pressure). Based on such experiments, it is possible to obtain insights into the thermodynamic differences (e.g. entropy, enthalpy and volume) between the two states. Increasing the hydrostatic pressure has been reported to be a very subtle way to shift populations of interchanging states as this minimally influences the free energy difference between the two states (thermodynamics).[7–8] At the same time, the applied pressure can alter the energy of transition states, which results in changes in the exchange rates between the states (kinetics). High pressure NMR applications are becoming increasingly popular, despite the technical challenges that are associated with applying hydrostatic pressure to an NMR sample.[9] A small and far from complete list of impressive pressure NMR studies include the study of folding intermediates for apomyoglobin,[10] the determination of the conformational equilibria for the β1-adrenergic GPCR,[11] the identification of allosteric mechanisms in the RAS protein[12] and the study of a β-strand register shift in the ARNT protein.[13] In addition, highly advanced pressure jumps equipment has been designed and dedicated NMR experiments have been developed.[14–19] These examples highlight the power and potential of using elevated pressure to reveal molecular details.

The effect that pressure has on the free energy difference between states A and B (at constant temperature) can, based on a Taylor expansion, be written as[8,20] $\Delta G_{AB} = \Delta G_0 + \Delta V_0(p - p_0) - 0.5\Delta\kappa_T(p - p_0)^2$, where $\Delta G_0$ and $\Delta V_0$ are, respectively, the free energy and the volume differences between states A and B at standard pressure (1 bar), $p$ and $p_0$ are the pressure and the standard pressure and $\Delta\kappa_T$ is the change in isothermal compressibility between states A and B. When the compressibility of states A and B is the same, the equilibrium constant changes with pressure according to $K_{eq} = exp\left(-\frac{\Delta G_0 + \Delta V_0(p-p_0)}{RT}\right)$. The determination of $K_{eq}$ at different pressures $p$ can thus provide direct insights into the difference of the molecular volume between states A and B ($\Delta V_0$).

Upon protein folding the volume of a protein tends to increase due to the formation of molecular cavities. A negative volume change ($\Delta V_0 = V_B - V_A$) is thus usually associated with a loss of secondary or tertiary structure. In accordance with that, high hydrostatic pressures will eventually result in the (partial) unfolding or denaturation of proteins.

Based on transition state theory it is possible to obtain insights into the free energy of activation through the Eyring equation $k = \frac{\kappa k_B T}{h} exp\left(-\frac{\Delta G^{\ddagger}}{RT}\right)$, where $k$ is the forward ($k_{AB}$) or reverse ($k_{BA}$) rate constant, $\kappa$ is the transmission coefficient, $k_B$ is the Boltzmann constant, $h$ is the Planck constant and $\Delta G^{\ddagger}$ is the free energy of activation that is associated with the forward ($\Delta G^{\ddagger}_{AB}$) or reverse ($\Delta G^{\ddagger}_{BA}$) rate. Including the dependence of the free energy on the pressure this expression can be rewritten as: $k = \frac{\kappa k_B T}{h} exp\left(-\frac{\Delta G^{\ddagger}_0 + \Delta V^{\ddagger}_0(p-p_0)}{RT}\right) = exp\left(ln(k_0) - \frac{\Delta V^{\ddagger}_0(p-p_0)}{RT}\right)$, where $k_0$ is the (forward $k_{0,AB}$ or reverse $k_{0,BA}$) rate at standard pressure. The pressure dependence of $k_{AB}$ and $k_{BA}$ thus provides insights into the volume differences between state A and the transition state or between state B and the transition state.

Carr–Purcell–Meiboom–Gill (CPMG) relaxation dispersion (RD) NMR experiments[21–22] can provide quantitative insights into $k_{AB}$ and $k_{BA}$ as well as $K_{eq}$. Even when the sparsely populated second state is not directly observable in NMR spectra, the exchange process between states A and B can be quantified based on the exchange broadening of the resonances of the majorly populated state A, e.g. by measuring the effective transverse relaxation rate as a function of CPMG frequency. Performing CPMG RD experiments at different pressures thus provides a means to obtain information on the volume differences between the ground state and an invisible protein conformation or the transition state. This information is highly valuable as it gives direct insights into the nature of the structural changes that occur in biomolecules. Indeed, previous work that quantified exchange processes using NMR methods has revealed unique insights into e.g. the enzymatic mechanisms from an adenylate kinase,[23] the two- and three-state folding pathways of the drnN, G48M Fyn[24] and A39V, N53P, V55L Fyn SH3 domains,[25] the structural properties of the transition-state ensemble of a mutant version of apocytochrome b562 that folds in a two state mechanism,[26] the destabilizing effect of cavities for the T4 lysozyme L99A protein,[27] the folding[28] and aromatic ring flipping[29] of GB1 and the folding of two domains of the ribosomal protein L9.[30] These high pressure NMR studies mainly focused on $^{15}N$ based RD experiments, which are suited for proteins up to a molecular weight of approximately 30 kDa, but fail for larger complexes due to very fast transverse relaxation rates that prevent the recording of NMR spectra with sufficient signal to noise. In the current work, we focus on the use of $^{13}CH_3$

methyl groups in an otherwise fully deuterated background that provide high quality spectra even for molecular machines that are far over 100 kDa.[31–36]

One of the complexes that is well studied using methyl TROSY[37] methods is the 45 kDa Dcp1:Dcp2 mRNA decapping complex.[38–40] This complex contains the Dcp1 decapping activator and the Dcp2 enzyme, that can be divided into a regulatory domain (RD, residues 1–95 in *S. pombe*), that is connected to the catalytic domain (CD, residues 96–243 in *S. pombe*) via a flexible linker, as well as a C-terminal intrinsically disordered extension. The Dcp2 regulatory and catalytic domains can adopt three different relative orientations. First, an auto-inhibited closed state, where the RD and CD interact in a non-productive manner and where the substrate RNA binding groove is inaccessible. Second, the open state, where the RD and CD do not interact and tumble independently. Third, the catalytically competent state, where the RD and CD interact such that the catalytic Nudix motif is in close spatial proximity to the mRNA cap structure and hydrolysis of the substrate can take place.[39,41] This catalytically competent state of the enzyme is only stably formed when mRNA substrate as well as the decapping activator Edc1 are recruited.[42] The Dcp2 enzyme is thus a highly dynamic protein that samples a complex energy landscape and in which the different states have different functions during catalysis. Based on CPMG RD experiments we established[39] that the apo Dcp1:Dcp2 complex mainly adopts the closed conformation ($p_{Closed}$ = 0.94)[43–44] in solution, whereas a small fraction adopts the open conformation ($p_{Open}$ = 0.06)[43] (Figure 1(**A**)). Previously we also determined that the closed and open conformation exchange at a rate ($k_{ex}$ = $k_{Closed\text{-}Open}$ + $k_{Open\text{-}Closed}$) of around 2800 $s^{-1}$.[39]

In this work, we exploit $^{13}C$ methyl group CPMG RD experiments on ILVMA labeled samples of the Dcp1:Dcp2 complex at different pressures. The pressure response of the Dcp1:Dcp2 dynamics was used to extract differences in the volume between the closed, the transition and the open state. Our work thereby reveals that high pressure NMR techniques can also be applied to molecular machines that are too large for $^{1}H$-$^{15}N$ based NMR spectroscopic approaches.

## Results

The Dcp1:Dcp2 mRNA decapping complex that we study here has a molecular weight of 45 kDa and the low quality $^{1}H$-$^{15}N$ NMR spectra do not allow for the recording of $^{15}N$ based NMR relaxation data, even upon full deuteration of the complex. For that reason, we make use of methyl TROSY methods[37] of spectroscopically isolated $^{1}H_3$-$^{13}C$ labeled methyl groups of isoleucine, leucine, valine, alanine and methionine residues in a per-deuterated background. These samples can be prepared through the use of dedicated precursor molecules that are incorporated into the protein of interest during over-expression in *E. coli*.[31,45–46] The NMR active methyl groups are excellent probes to study the dynamics within the decapping complex.[39] To simplify the NMR spectra we restricted the methyl group labeling to the Dcp2 enzyme, while the Dcp1 protein was present in an NMR invisible form.

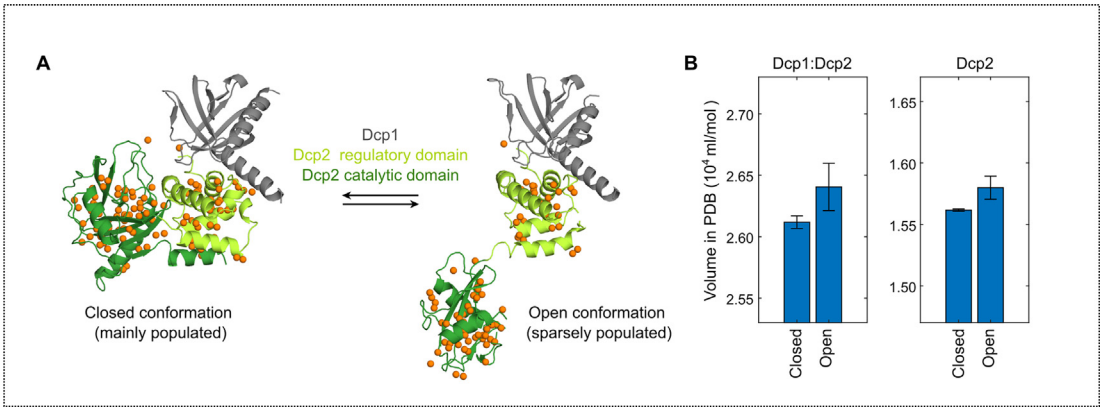


**Figure 1.** Structure and dynamics in the Dcp1:Dcp2 mRNA decapping complex. (A) Structure of the Dcp1:Dcp2 complex, that can adopt a closed (left) and an open (right) conformation. Dcp1 is colored grey, the Dcp2 regulatory domain in light green and the Dcp2 catalytic domain in dark green. The regulatory and catalytic domain of Dcp2 are in direct contact in the closed state. The NMR methyl probes of isoleucine, leucine, valine, alanine and methionine residues are shown as orange spheres. (B) The calculated[47] volumes of the closed and open conformations of Dcp1:Dcp2 (left) and Dcp2 (right) based on the crystal structure of the complex[43] (PDB ID: 2qkm). The error bars indicate the standard deviations and are based on the structures of the two closed and two open conformations of the complex in the crystal structure, respectively.

Two copies of the closed and open conformations are present in a crystal structure of the Dcp1:Dcp2 complex that was determined in the presence of ATP.[43] To assess if pressure can potentially be used to modulate the equilibrium between the open and the closed conformation we calculated the molecular volumes[47] of both states (Figure 1(**B**)). This simple calculation suggests that the transition from the closed to the open conformation is not associated with a significant change in molecular volume ($p > 0.1$).

To experimentally follow the pressure response of the Dcp1:Dcp2 complex with high spatial resolution we recorded methyl TROSY NMR spectra between 10 and 2750 bar (1 to 275 MPa) (Figure 2(**A**)). Increasing the experimental pressure resulted in a global and gradual shift of the methyl group resonances, as is expected based on experiments with model peptides.[48] The extent and direction of the chemical shift perturbations (CSPs), however, differed from residue to residue. Previously, the non-linearity of pressure induced CSPs has been linked to the presence of internal cavities in proteins.[13,49–51] In Dcp2, we observe this behavior for a number of resonances (Figure 2(**B**)), indicating that the corresponding residues are close to internal voids that are compressed at elevated pressure. In addition, we observe that a number of resonances disappear when the pressure exceeds 750 bar. Also this behavior has been linked to pressure induced conformational fluctuations around protein cavities.[52] Taken together, these data indicate that Dcp2 contains internal cavities and/or that Dcp2 undergoes conformational rearrangements that are pressure dependent. Next, we calculated the location of the cavities within Dcp2 based on the structure of the enzyme in the closed conformation. We found that the interface between the N-terminal regulatory and the C-terminal catalytic domain, that changes upon the closed to open transition, contains voids in the closed conformation (Figure 2 (**C**)). Interestingly, most of the resonances that either disappear or that shift non-linearly are from residues that are in close spatial proximity to this region (Figure 2(**C**)).

We noticed that Dcp1:Dcp2 is not stable for extended times at pressures that exceed 600 bar, likely due to partial destabilization of the complex that results in denaturation. For our subsequent experiments we thus limited our measurements to relatively low hydrostatic pressures between 10 and 600 bar. Interestingly, we noted that the signals of M164 and M221 shift with respect to the other resonances (Figure 3(**A**), top left panel) at elevated pressure. Previously, we have shown that these methyl groups directly report on the conformational equilibrium between the closed and the open conformation in Dcp2.[39] As the exchange between the closed and open positions is fast on the NMR timescale, the population of both states can be approximately extracted from the resonance positions. In our high pressure experiments, the resonance frequencies of M164 and M221 are, however, influenced by two effects: on the one hand directly by the applied hydrostatic pressure and on the other hand indirectly by a shift in the conformational equilibrium. To disentangle these effects, we also recorded methyl TROSY spectra of the Dcp2 C-terminal catalytic domain at the same elevated pressures. The resonances of this Dcp2 fragment

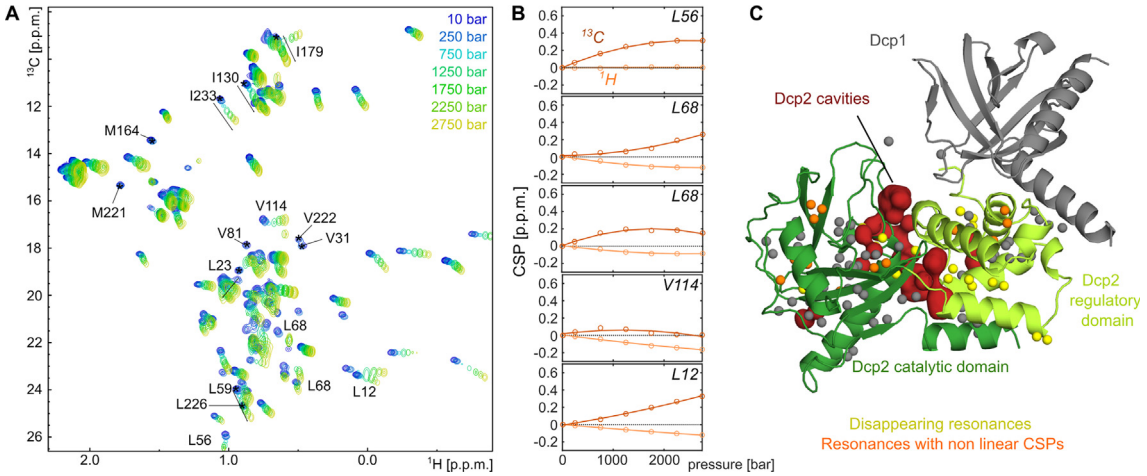


**Figure 2.** Pressure induced chemical shift perturbation of the methyl groups in Dcp2. (A) $^{1}$H-$^{13}$C methyl TROSY spectra of the Dcp1:Dcp2 decapping complex, where Dcp2 is NMR active in the ILVMA methyl groups, whereas Dcp1 is NMR invisible. (B) Examples for non-linear pressure dependent chemical shift changes. Dark and light orange lines and data points correspond to the $^{13}$C, respectively the $^{1}$H direction. (C) Structure of the Dcp1:Dcp2 complex in the closed conformation, colored as in Figure 1(**A**). The residues for which the NMR resonances disappear or that experience non-linear chemical shift perturbations are marked in yellow and orange respectively. The calculated major cavities in Dcp2 are indicated with a red surface.

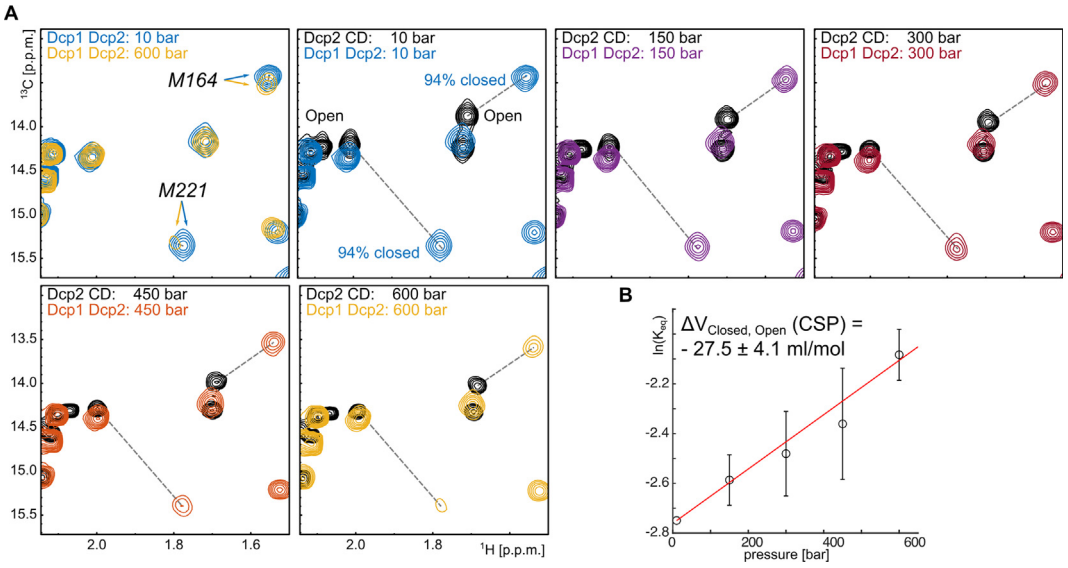


**Figure 3.** High pressure results in a shift of the populations towards the open state. (A) Methionine region of methyl TROSY spectra of the Dcp1:Dcp2 complex at different pressures between 10 and 600 bar (colored contours) and of the Dcp2 catalytic domain (black). The dashed lines indicate the shift of the methyl resonances of M164 and M221 between the open state (black contours) and the equilibrium of the states that are sampled by the Dcp1:Dcp2 complex. The spectra in the top left panel were shifted manually based on resonances that are remote from the Dcp2 RD CD interface, to compensate for the global pressure induced chemical shift perturbations. The arrows in the top left panel highlight the shift of the complex towards the open state. (B) Increasing the pressure results in a shift towards the open state, from which the volume difference between the closed and the open state was derived.

correspond to the fully open conformation of Dcp1:Dcp2, as the Dcp2 N-terminal regulatory domain and Dcp1, that are needed for the formation of the closed Dcp2 conformation, are missing. For all pressures we then calculated the distance between the M164 and M221 open-state chemical shift (based on the Dcp2 C-terminal catalytic domain) and the chemical shift for those residues in the Dcp1:Dcp2 complex (closed to 94%; $\ln(K_{eq})$ = -2.75) (Figure 3(**A**)). Based on the assumption that the chemical shift difference between the open and the closed state is independent of pressure in the limited pressure range that we use here, we derived the equilibrium constants at the elevated pressures and noticed that these increase ($\ln(K_{eq})$ increases). For increased pressures a shift of the conformational equilibrium towards the open conformation thus takes place, revealing that the open conformation has a smaller molecular volume than the closed conformation. Based on the dependency of $K_{eq}$ on pressure we derived a volume difference between the closed and the open conformation of $-27.5 \pm 4.1$ ml/mol ($-45.5 \pm 6.8$ Å$^3$) (Figure 3 (**B**)). This is in agreement with the void volumes that are secluded at the interface between the regulatory and catalytic domains in the closed conformation of the complex (Figure 2(**C**)), but contradicts the simple overall volume calculations that we performed (Figure 1(**B**)).

To independently confirm this result and to obtain insights into the volume differences between the transition state structure and the closed, respectively the open conformation, we turned to $^{13}$C single quantum (SQ) CPMG RD experiments at the different pressures. We found that five different methyl groups from 4 residues that are located at the interface between the Dcp2 regulatory and catalytic domain show clear RD profiles that can be analyzed at all pressures. To analyze these data we first determined the chemical shift difference between the closed and the open states based on the NMR resonances of the Dcp1:Dcp2 complex (94% closed) and the Dcp2 catalytic domain (open) (Figure 4(**A**)). At a pressure of 10 bar, we could then fit the CPMG RD data to one global two state exchange process and obtained a forward rate ($k_{Closed \rightarrow Open}$) of $155 \pm 26$ s$^{-1}$ and a backward rate ($k_{Open \rightarrow Closed}$) of $3280 \pm 200$ s$^{-1}$, and thus a $K_{eq}$ of $0.047 \pm 0.005$ (Figure 4(**B**), Table 1). This is in reasonably good agreement with previous exchange parameters ($k_{Closed \rightarrow Open} \sim 170$ s$^{-1}$ and $k_{Open \rightarrow Closed} \sim 2650$ s$^{-1}$) that were extracted from data that was recorded at ambient pressure and on a sample where the methyl labeling was restricted to the isoleucine and methionine residues.[39]

Next, we performed CPMG RD dispersion measurements at 150, 300, 450 and 600 bar. We analyzed the CPMG RD curves for five methyl groups at five different pressures simultaneously (Figure 4(**B**)), assuming that the chemical shift difference between the two states was

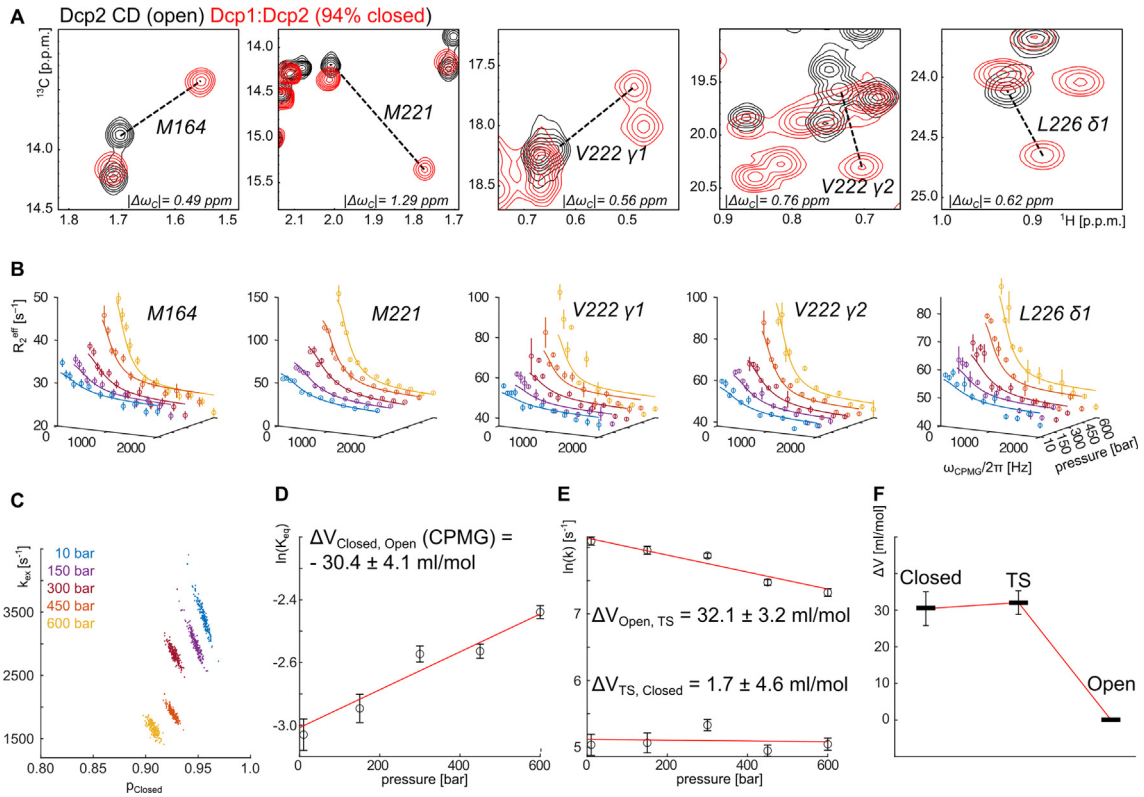


**Figure 4.** Volumetric properties of the Dcp1:Dcp2 complex. (A) Overlay of the NMR spectra of the Dcp1:Dcp2 complex (red; 94% closed) and the Dcp2 catalytic domain (CD; black, 100% open). The derived chemical shift differences between the two states are indicated. (B) $^{13}$C SQ CPMG RD curves for 5 methyl groups at 5 different pressures. The data points are indicated with circles, vertical lines indicate error bars that represent the standard deviation derived from two independent measurements. The drawn lines are a global fit of the data to a two-site exchange model. (C) Distribution of $p_{Closed}$ and $k_{ex}$, for the different pressures, derived from 250 fitting cycles where the experimental data was randomly varied according to the experimental error. (D) Pressure dependence of the equilibrium constant and the derived volume difference between the closed and the open state. (E) Pressure dependence of the forward (closed to open; bottom) and reverse (open to closed; top) rates that were used to determine the volume differences between the closed or the open conformation and the transition state. (F) Volume changes of Dcp1:Dcp2 during the transition from the closed to the open state. TS: transition state. The error bar shown for the closed state corresponds to the standard deviation of the volume difference between the closed and the open state (panel D), the error bar shown for the TS corresponds to the standard deviation of the volume difference between the open state and the TS (panel E).

Table 1 Exchange parameters for the Dcp1:Dcp2 and the Dcp1:Dcp2:ATP complexes at different pressures.

| | **Dcp1:Dcp2** | | **Dcp1:Dcp2:ATP** | |
|---|---|---|---|---|
| pressure (bar) | $p_{Closed}$ | $k_{ex}$ ($s^{-1}$) | $p_{Closed}$ | $k_{ex}$ ($s^{-1}$) |
| 10 | 0.955 (±0.004)* | 3434 (±227) | 0.951 (±0.003) | 2870 (±104) |
| 150 | 0.947 (±0.005) | 3018 (±201) | 0.940 (±0.003) | 2708 (±109) |
| 300 | 0.927 (±0.004) | 2841 (±112) | 0.920 (±0.002) | 2718 (±67) |
| 450 | 0.926 (±0.003) | 1903 (±89) | 0.878 (±0.004) | 2985 (±113) |
| 600 | 0.907 (±0.004) | 1671 (±99) | 0.880 (±0.004) | 2333 (±71) |

* The indicated errors are based on a bootstrap error analysis, where the data was resampled and refitted 250 times.

independent of the hydrostatic pressure. Our analysis revealed that elevated pressures resulted in a shift towards the open conformation (Figure 4 (**C**), Table 1), from which we extracted that the volume difference between the closed and open conformation ($V_{Open}$-$V_{Closed}$) is −30.4 ± 4.1 ml/mol (Figure 4(**D**), Table 1). This finding is in good agreement with the volume difference that was determined from the resonance position in the NMR spectra (Figure 3(**B**)) and thus independently confirms that the open conformation has a smaller molecular volume than

the closed state due to the loss of voids at the interface between the Dcp2 catalytic and regulatory domains. Based on the changes in $k_{Closed \rightarrow Open}$, and $k_{Open \rightarrow Closed}$ with pressure (Figure 4(**E**)), we determined that the volume of the transition state is similar to the volume of the closed conformation (Figure 4(**F**)). It is tempting to speculate that also the structure of the transition state is similar to the structure of the closed state. In that case, the opening pathway of the complex could be initiated by a reshuffling of the interface contacts that subsequently results in the dissociation of the Dcp2 regulatory and catalytic domains. Tryptophan 43 might be a central residue in the initial steps of the opening of the Dcp2 enzyme. This residue is located in the middle of the RD-CD interface and has been shown to play an important role in stabilizing the closed conformation.[40]

ATP binding has been suggested to stabilize the closed conformation of Dcp1:Dcp2.[39,43] We therefore added 10 mM of this nucleotide to the Dcp1:Dcp2 complex. This resulted in CSPs for a number of methyl group resonances in the catalytic domain of Dcp2 that are located around the Box B region that interacts with the mRNA body of the substrate (Figure 5(**A**)). We next performed the ATP titration with the isolated catalytic domain that mimics the open conformation (Figure 5(**B**)). In this case we observed larger CSPs that localize to a region that includes the C-terminal end of the Nudix helix that is important for the recognition of the capped mRNA substrate. Interestingly, neither the ATP induced CSPs in the closed (Dcp1:Dcp2) state nor the CSPs in the open (CD) state agree very well with the site where ATP binding has been observed in the crystal structure of the complex (Figure 5(**A**)). Based on these findings we conclude that ATP can interact with the mRNA decapping complex in multiple ways and that the interaction mode depends on the conformation of the complex.

An ATP induced shift in the closed-open equilibrium would be directly observable in RD CPMG experiments, where an increase in the population of the closed state from e.g. 94 to 97% would result in a ~50% reduction of the amplitude of the RD curves. We noticed, however, that the amplitudes of the CPMG RD curves are almost insensitive to the addition of ATP (Figure 5(**C**)). This finding shows that ATP does not significantly shift the populations towards the closed (or open) conformation under the experimental conditions

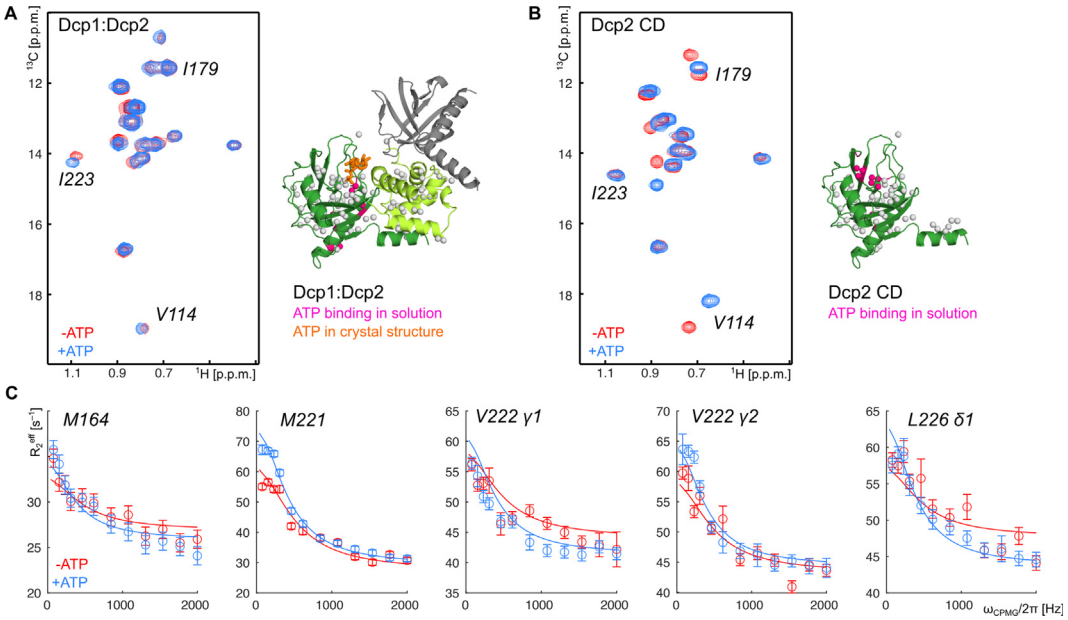


**Figure 5.** Binding of ATP to the Dcp2 catalytic domain. (A) Overlay of the methyl TROSY spectrum of Dcp1:Dcp2 in the absence (red) and presence (blue) of ATP. The residues that experience the strongest chemical shift perturbations upon addition of ATP are highlighted in pink on the structure of the closed conformation of the complex. The bound ATP in the crystal structure is shown in orange. (B) Overlay of the methyl TROSY spectra of the Dcp2 catalytic domain (CD) in the absence (red) and presence (blue) of ATP. The residues that experience the strongest chemical shift perturbations upon addition of ATP are highlighted in pink on the structure of the domain. (C) $^{13}C$ SQ CPMG relaxation curves for five methyl groups at the interface between the Dcp2 regulatory and catalytic domains in the absence (red) and presence (blue) of ATP. The addition of ATP has a minor influence on the amplitude of the RD curves, indicating that the addition of ATP does not result in a shift of the equilibrium between the closed and open states. The data points are indicated with circles, vertical lines indicate error bars that represent the standard deviation derived from two independent measurements. The drawn lines are a global fit of the data to a two-site exchange model as described in Figures 4 and 6.

that we used here. To fit the CPMG RD curves in the presence of ATP we used the chemical shift differences between the Dcp1:Dcp2:ATP complex (94% closed) and the Dcp2 catalytic domain:ATP complex (open) (Figure 6(**A**)). Interestingly, the changes in $|\Delta\omega c|$ due to ATP binding (Figures 4 (**A**) and 6(**A**)) can to a large degree explain the changes in the CPMG RD curves (Figure 5(**C**)) at ambient pressure.

Subsequently we increased the pressure in a stepwise manner and recorded CPMG RD curves on the Dcp1:Dcp2:ATP complex. Like for the apo complex, we fitted the data of all pressures simultaneously, assuming that the chemical shift differences between the open and closed state are pressure independent between 10 and 600 bar (Figure 6(**B**), Table 1). With pressure, we observed a gradual shift of the populations towards the open state (Figure 6(**C**)), from which we extracted a volume difference of −41.0 ± 2.3 ml/mol (Figure 6(**D**)). Compared to the complex without ATP, the change in molecular volume is thus larger. The changes in the forward and reverse rates with pressure (Figure 6(**E**)) reveal that the volume of the transition state now lies in-between the volumes of the closed and open state (Figure 6(**F**)).

## Concluding remarks

Many conformations that a protein can adopt are not directly detectable due to their low abundance. Knowledge about the nature of these states is, however, important as they can be catalytically important and as (local) unfolding may result in protein aggregation or mis-folding that can have a severe impact on cellular homeostasis. NMR methods are very well suited to obtain information about invisible minor states from resonances of the visible major state.[53–55] Importantly, this infor-

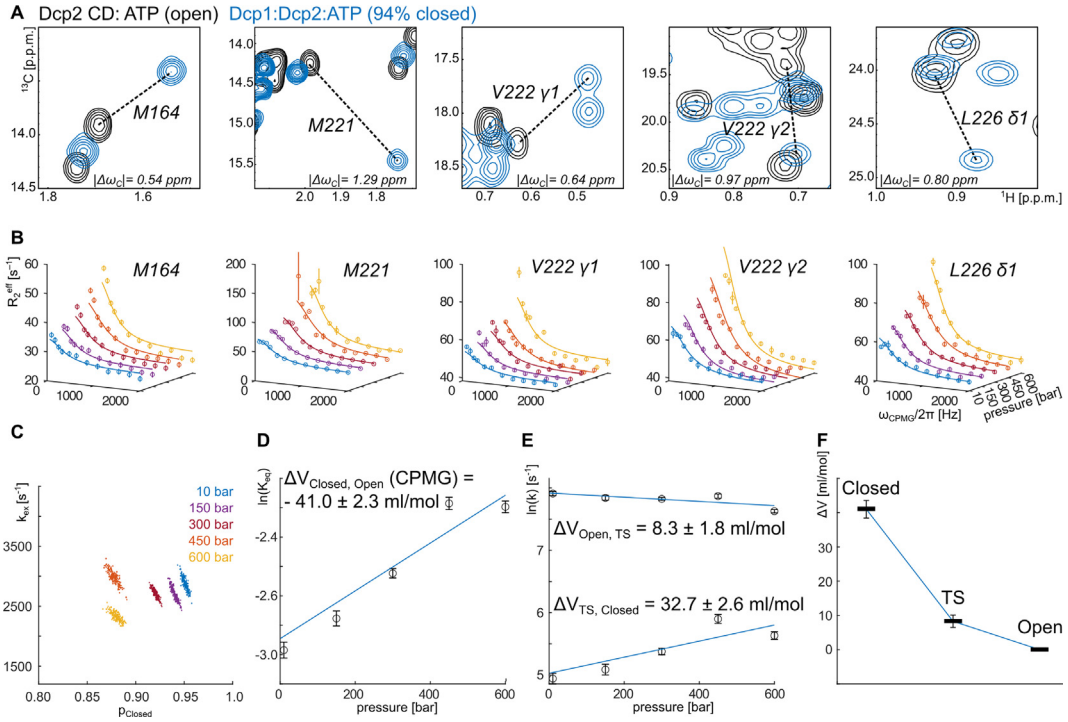


**Figure 6.** Pressure dependent CPMG RD dispersion experiments of the Dcp1:Dcp2:ATP complex. (A) Overlay of the NMR spectra of the Dcp1:Dcp2:ATP complex (blue; 94% closed) and the Dcp2 catalytic domain in complex with ATP (CD; black, 100% open). The derived chemical shift differences between the two states are indicated. (B) $^{13}C$ SQ CPMG RD curves for five methyl groups at five different pressures. The data points are indicated with circles, the error bars represent the standard deviation derived from two independent measurements. The drawn lines are a global fit of the data to a two-site exchange model. (C) Distribution of $p_{Closed}$ and $k_{ex}$, for the different pressures derived from 250 fitting cycles where the experimental data were randomly varied according to the experimental error. (D) Pressure dependence of the equilibrium constant and the derived volume difference between the closed and the open state. (E) Pressure dependence of the forward (closed to open; bottom) and reverse (open to closed; top) rates and the derived volume differences between the closed or the open state and the transition state. (F) Volume changes of Dcp1:Dcp2:ATP during the transition from the closed to the open state. The error bar shown for the closed state corresponds to the standard deviation of the volume difference between the closed and the open state (panel D), the error bar shown for the TS corresponds to the standard deviation of the volume difference between the open state and the TS (panel E).

mation can be obtained with a very high spatial resolution.

In summary, we here studied how the Dcp1:Dcp2 complex exchanges between a closed and an open conformation. Based on $^{13}C$ SQ CPMG RD experiments at different pressures, we extracted information about the volume changes along the closing-opening pathway of the complex. Our data is in agreement with a model in which the opening of the apo complex first involves local rearrangements of the interface residues without changing the overall shape of the complex, before both domains then dissociate into the fully open conformation. In the presence of ATP, the volume of the complex changes in a stepwise manner. This is in agreement with a situation where the interactions between ATP and the Dcp2 CD change when the complex shifts into the open conformation. Interestingly, we observe such a change of the Dcp2:ATP interactions in our NMR titrations, where the Dcp1:Dcp2 complex binds ATP via the Box B region and where the Dcp2 CD interact with ATP via a region next to the Nudix domain (Figure 5(**A**) and (**B**)).

It is worth noting that the experimentally determined changes in the molecular volume between the closed and open state could not be reliably extracted from known static crystal structures (Figure 1(**B**)), which highlights the importance of the methodology that we exploited here. Our combination of methyl labeling and high pressure NMR methods provides the means to obtain unique insights into the volumetric properties of large molecular machines.

## Materials and methods

### Transformation and protein expression

*E. coli* BL21(DE3) Codon PlusRIL cells (Stratagene) were transformed with a pET derived plasmid that encodes the Dcp1 (residues 1–127; UniprotID: Q9P805, internal ID: 43), Dcp2 (residues 1–243; UniprotID: O13828; internal ID: 223) or Dcp2 (residues 96–243; internal ID: 222) proteins from *S. pombe*. All proteins contained an N-terminal His6-TEV tag to aid purification. Cells were grown in the presence of 50 mg/L kanamycine and 34 mg/L chloramphenicol in an incubator shaker at 37 °C. Dcp1 was prepared in a partially (~80%) deuterated form by making use of an M9 minimal medium that was based on 90–95% $D_2O$ and protonated glucose. Dcp2 was prepared in a per-deuterated form by making use of an M9 medium that contained 100% $D_2O$ and $^{2}H$, $^{12}C$-glucose (2 g/L). NMR active ($^{13}CH_3$) methyl groups were introduced into the Dcp2 protein at the isoleucine-δ1, leucine-δ, valine-ɣ, methionine-ε and alanine-β positions. To that end, 60 mg/L 2-ketobutyric acid-4-$^{13}C$,3,3-$^{2}H_2$, 100 mg/L 2-Keto-(3-methyl- $^{13}C$)-butyric acid-4-$^{13}C$,3- $^{2}H$ and 100 mg/L L-Methionine-(methyl- $^{13}C$) were added to the cells at an $OD_{600}$ of 0.6–0.8. 40 minutes later, 100 mg/L L-Alanine-3- $^{13}C$,2- $^{2}H$ was added. 20 minutes later protein expression was induced with 1 mM IPTG. Protein production took place at 20 °C for 10–15 hours, after which the cells were harvested by centrifugation and stored at −20 °C.

### Protein purification

Cell pellets were solubilized in ice-cold lysis buffer (400 mM NaCl, 50 mM sodium phosphate, pH 7.4, 10 mM imidazole) supplemented with 0.1% Triton X-100, 200 μg/mL lysozyme and 1 μg/mL DNase I. Cells were lysed by sonication on ice and the cell lysate was cleared by centrifugation. The supernatant was applied to an NiNTA-column that was equilibrated with lysis buffer. The column was washed with 10 column volumes of lysis buffer, 5 column volumes of wash buffer A (1 M NaCl, 50 mM sodium phosphate, pH 7.4) and 10 column volumes of wash buffer B (400 mM NaCl, 50 mM sodium phosphate, pH 7.4, 30 mM imidazole). The target protein was eluted from the column using elution buffer (150 mM NaCl, 50 mM sodium phosphate, pH 7.4 and 300 mM imidazole). The eluted protein was dialysed overnight against dialysis buffer (150 mM NaCl, 25 mM sodium phosphate, pH 7.4 and 1 mM DTT) in the presence of TEV protease to remove the $His_6$ affinity tag. The $His_6$ tag and the TEV protease were removed from the target protein by applying the dialysed solution to a NiNTA-column that was equilibrated in dialysis buffer. The Dcp1:Dcp2 decapping complex was subsequently formed by mixing both proteins in a 3:2 ratio. The excess of Dcp1 was removed during a final size exclusion chromatography step (Superdex 75; GE Healthcare) in size exclusion buffer (125 mM NaCl, 25 mM HEPES, pH 7.3 and 1 mM DTT). The Dcp1:Dcp2 complex was subsequently concentrated and exchanged into NMR buffer (125 mM NaCl, 25 mM HEPES, pD 7.3 and 1 mM DTT in 100% $D_2O$) using a spin concentrator. Protein concentrations were determined by measuring their absorption at 280 nm. For the Dcp1:Dcp2:ATP complex an ATP concentration of 10 mM was used. This high ATP concentration was used to ensure saturation of the ATP binding site such that ligand exchange will not result in CPMG relaxation dispersions.

### NMR measurements

All NMR measurements were performed on a Bruker NEO spectrometer that operated at a proton frequency of 500 (Dcp2 catalytic domain; nitrogen cooled TCI probehead) or 800 (Dcp1:Dcp2 complexes; helium cooled TCI probehead) MHz at 303 K. For measurements at standard pressure (1 bar) a 500 μl sample volume was used. Measurements at higher pressure levels

were performed using a special high pressure system consisting of a ceramic cell (Daedalus Innovations LLC) that holds 250 μl sample and a PBI Pressure Hub (Pressure BioSciences Inc, MA) which is synchronized with the spectrometer and allows for automatic pressure control and the recording of automatic pressure series. The NMR buffer contained 125 mM NaCl, 25 mM HEPES, pD 7.3 and 1 mM DTT in 100% $D_2O$. In addition, 50 μM DSS was added for referencing. NMR samples had a protein concentration between 170 and 300 μM for high pressure relaxation dispersion experiments and between 50 and 80 μM for methyl TROSY (HMQC) experiments. Spectra processing was done with the NMRPipe/NMRDraw software.[56]

### Chemical shift assignments

The chemical shifts of the isolated Dcp2 catalytic domain were assigned based on assignments of Dcp2 in the Dcp1:Dcp2 complex, on a 3-dimensional (H)-C-C-H NOESY experiment (mixing time 400 ms) that was recorded on the Dcp2 CD and on the known structure of the CD.[43] NOESY experiments were visualized and manually analyzed using CARA (cara.nmr.ch).

### Relaxation dispersion measurements

$^{13}C$ single quantum Carr–Purcell-Meiboom–Gill relaxation dispersion experiments[57] were performed at 800 MHz proton frequency with CPMG frequencies of 77, 154, 231, 308, 462, 615, 846, 1077, 1308, 1538, 1769, 2000 Hz and a relaxation delay of 26 ms. Peaks were picked and integrated using the NMRPipe/NMRDraw software.[56] Intensities were converted into relaxation rates and RD curves were fitted numerically using in-house Matlab scripts which are based on the exact analytic equations presented by Baldwin.[58] Fitting was performed simultaneously for the methyl groups of Met221, M164, V222 ($\gamma$1 and $\gamma$2) and L226 ($\delta$1), that could be analyzed at all pressures in the absence and presence of ATP. It was assumed that $|\Delta\omega_C|$ was independent of the applied pressure. The $|\Delta\omega_C|$ value was fixed for each methyl group based on the resonance frequency of the methyl group in the Dcp2 catalytic domain (fully open conformation) and the resonance frequency in the Dcp1:Dcp2 or Dcp1:Dcp2:ATP complex (94% closed conformation). It is important to note that the extracted volume changes were indistinguishable when assuming that the Dcp1:Dcp2 or Dcp1:Dcp2:ATP complexes at ambient pressure were either 90 or 98% closed. Errors in the individual relaxation rates were determined based on duplicate measurements and were assumed to have a standard deviation of at least 1 Hz. Errors in the extracted exchange parameters were obtained from refitting the data 250 times after randomly varying the experimentally determined relaxation rates based on the errors in these rates. In that process the starting parameters for the minimization were randomly varied by 10%. The volume changes were obtained by simultaneously fitting the pressure dependence of the determined equilibrium constant as well as the forward and reverse rates using the Eyring relationship. It is worth noting that the CPMG data and the pressure dependence of the rates could also be well fitted at the same time, which yielded highly similar volume changes (i.e. enforcing the CPMG fitting parameters to obey the Eyring equation).

### Protein cavities, volumes and images

Protein voids were located using the program HOLLOW,[59] based on the Dcp2 protein in the closed conformation (PDB ID: 2QKM, chain B) that was energy minimized in Chimera[60] using the command “Minimize Structure”. Internal cavities were separated from surface cavities by manual inspection in Pymol (The PyMOL Molecular Graphics System, Version 2.0 Schrödinger, LLC.). Protein volumes were calculated using the program ProteinVolume.[47] To that end, the coordinates of the 2 open and 2 closed conformations of Dcp1:Dcp2 were extracted from the PDB (PDB ID: 2QKM, chains A/B, C/D, E/F and G/H), protons were added to the model using the Chimera[60] command “AddH”, after which the structural models were minimized in Chimera using the command “Minimize Structure”, based on the default settings. For the comparison of the volumes of the open and closed conformations of Dcp2 and Dcp1:Dcp2 (2 crystallographically independent copies of each conformation are present in the crystal) only the atoms that are present in all models (PDB ID: 2QKM) were considered and all ligand atoms were removed. Protein images were prepared using Pymol.

***CRediT authorship contribution statement.*** **Christina Krempl:** Formal analysis, Investigation, Methodology, Software, Visualization, Writing – review & editing. **Jan Philip Wurm:** Conceptualization, Investigation, Methodology, Supervision, Writing – review & editing. **Markus Beck Erlach:** Methodology, Writing – review & editing. **Werner Kremer:** Conceptualization, Methodology, Resources, Supervision, Writing – review & editing. **Remco Sprangers:** Conceptualization, Formal analysis, Funding acquisition, Methodology, Project administration, Supervision, Validation, Writing – original draft, Writing – review & editing.

## DATA AVAILABILITY

Data will be made available on request.

## Acknowledgements

We thank Johanna Stöfl for excellent technical assistance. We thank Hans Robert Kalbitzer for providing access to the high pressure NMR setup. We acknowledge Jan Overbeck for suggestions as well as for support in fitting the CPMG RD data. We thank David Stelzig as well as all other members of the NMR group for discussions. This work was supported by the Deutsche Forschungsgemeinschaft under SFB 960 TP/B12 (to R.S.) and priority program FOR1979 (to W.K.)

## Declaration of Competing Interest

The authors declare that they have no known competing financial interests or personal relationships that could have appeared to influence the work reported in this paper.

*Received 19 October 2022;*
*Accepted 11 December 2022;*

***Keywords***:
methyl TROSY;
CPMG relaxation dispersion;
protein dynamics;
high pressure;
Dcp1:Dcp2 mRNA decapping complex

## References

1. Blundell, T.L., Wright, P.E., (2022). Structural Biology – Painting the Mechanistic Landscape of Biomolecules. *J. Mol. Biol.* **434**, https://doi.org/10.1016/j.jmb.2022.167566 167566.
2. Overbeck, J.H., Stelzig, D., Fuchs, A.-L., Wurm, J.P., Sprangers, R., (2022). Observation of conformational changes that underlie the catalytic cycle of Xrn2. *Nat. Chem. Biol.* **18**, 1152–1160. https://doi.org/10.1038/s41589-022-01111-6.
3. Wurm, J.P., Sung, S., Kneuttinger, A.C., Hupfeld, E., Sterner, R., Wilmanns, M., Sprangers, R., (2021). Molecular basis for the allosteric activation mechanism of the heterodimeric imidazole glycerol phosphate synthase complex. *Nat. Commun.* **12**, 2748. https://doi.org/10.1038/s41467-021-22968-6.
4. Oyen, D., Fenwick, R.B., Aoto, P.C., Stanfield, R.L., Wilson, I.A., Dyson, H.J., Wright, P.E., (2017). Defining the Structural Basis for Allosteric Product Release from *E. coli* Dihydrofolate Reductase Using NMR Relaxation Dispersion. *J. Am. Chem. Soc.* **139**, 11233–11240. https://doi.org/10.1021/jacs.7b05958.
5. Bhabha, G., Lee, J., Ekiert, D.C., Gam, J., Wilson, I.A., Dyson, H.J., Benkovic, S.J., Wright, P.E., (2011). A Dynamic Knockout Reveals That Conformational Fluctuations Influence the Chemical Step of Enzyme Catalysis. *Science* **332**, 234–238. https://doi.org/10.1126/science.1198542.
6. Stafford, K.A., Trbovic, N., Butterwick, J.A., Abel, R., Friesner, R.A., Palmer, A.G., (2015). Conformational Preferences Underlying Reduced Activity of a Thermophilic Ribonuclease H. *J. Mol. Biol.* **427**, 853–866. https://doi.org/10.1016/j.jmb.2014.11.023.
7. Kitahara, R., Akasaka, K., (2003). Close identity of a pressure-stabilized intermediate with a kinetic intermediate in protein folding. *PNAS* **100**, 3167–3172. https://doi.org/10.1073/pnas.0630309100.
8. Akasaka, K., (2006). Probing Conformational Fluctuation of Proteins by Pressure Perturbation. *Chem. Rev.* **106**, 1814–1835. https://doi.org/10.1021/cr040440z.
9. Sprangers, R., (2021). High-pressure NMR measurements provide insights into the different structural states that proteins can adopt. *Biophys. J .* **120**, 749–751. https://doi.org/10.1016/j.bpj.2021.01.014.
10. Kitahara, R., Yamada, H., Akasaka, K., Wright, P.E., (2002). High Pressure NMR Reveals that Apomyoglobin is an Equilibrium Mixture from the Native to the Unfolded. *J. Mol. Biol.* **320**, 311–319. https://doi.org/10.1016/S0022-2836(02)00449-7.
11. Abiko, L.A., Grahl, A., Grzesiek, S., (2019). High Pressure Shifts the $\beta_1$-Adrenergic Receptor to the Active Conformation in the Absence of G Protein. *J. Am. Chem. Soc.* **141**, 16663–16670. https://doi.org/10.1021/jacs.9b06042.
12. Kalbitzer, H.R., Rosnizeck, I.C., Munte, C.E., Narayanan, S.P., Kropf, V., Spoerner, M., (2013). Intrinsic Allosteric Inhibition of Signaling Proteins by Targeting Rare Interaction States Detected by High-Pressure NMR Spectroscopy. *Angew. Chem. Int. Ed.* **52**, 14242–14246. https://doi.org/10.1002/anie.201305741.
13. Xu, X., Gagné, D., Aramini, J.M., Gardner, K.H., (2021). Volume and compressibility differences between protein conformations revealed by high-pressure NMR. *Biophys. J.* **120**, 924–935. https://doi.org/10.1016/j.bpj.2020.12.034.
14. Kremer, W., Arnold, M., Munte, C.E., Hartl, R., Beck Erlach, M., Koehler, J., Meier, A., Kalbitzer, H.R., (2011). Pulsed Pressure Perturbations, an Extra Dimension in NMR Spectroscopy of Proteins. *J. Am. Chem. Soc.* **133**, 13646–13651. https://doi.org/10.1021/ja2050698.
15. Roche, J., Dellarole, M., Caro, J.A., Norberto, D.R., Garcia, A.E., Garcia-Moreno, B., Roumestand, C., Royer, C.A., (2013). Effect of Internal Cavities on Folding Rates and Routes Revealed by Real-Time Pressure-Jump NMR Spectroscopy. *J. Am. Chem. Soc.* **135**, 14610–14618. https://doi.org/10.1021/ja406682e.
16. Alderson, T.R., Charlier, C., Torchia, D.A., Anfinrud, P., Bax, A., (2017). Monitoring Hydrogen Exchange During Protein Folding by Fast Pressure Jump NMR Spectroscopy. *J. Am. Chem. Soc.* **139**, 11036–11039. https://doi.org/10.1021/jacs.7b06676.
17. Charlier, C., Courtney, J.M., Alderson, T.R., Anfinrud, P., Bax, A., (2018). Monitoring 15N Chemical Shifts During Protein Folding by Pressure-Jump NMR. *J. Am. Chem. Soc.* **140**, 8096–8099. https://doi.org/10.1021/jacs.8b04833.
18. Charlier, C., Courtney, J.M., Anfinrud, P., Bax, A., (2018). Interrupted Pressure-Jump NMR Experiments Reveal Resonances of On-Pathway Protein Folding Intermediate. *J. Phys. Chem. B* **122**, 11792–11799. https://doi.org/10.1021/acs.jpcb.8b08456.
19. Charlier, C., Alderson, T.R., Courtney, J.M., Ying, J., Anfinrud, P., Bax, A., (2018). Study of protein folding under native conditions by rapidly switching the hydrostatic pressure inside an NMR sample cell. *PNAS* **115** https://doi.org/10.1073/pnas.1803642115.

20. K. Akasaka, H. Matsuki (Eds.), High Pressure Bioscience: Basic Concepts, Applications and Frontiers, Springer Netherlands, Dordrecht, 2015. https://doi.org/10.1007/978-94-017-9918-8.
21. Palmer, A.G., (2015). Enzyme Dynamics from NMR Spectroscopy. *Acc. Chem. Res.* **48**, 457–465. https://doi.org/10.1021/ar500340a.
22. Korzhnev, D.M., Kay, L.E., (2008). Probing Invisible, Low-Populated States of Protein Molecules by Relaxation Dispersion NMR Spectroscopy: An Application to Protein Folding. *Acc. Chem. Res.* **41**, 442–451. https://doi.org/10.1021/ar700189y.
23. Stiller, J.B., Jordan Kerns, S., Hoemberger, M., Cho, Y.-J., Otten, R., Hagan, M.F., Kern, D., (2019). Probing the transition state in enzyme catalysis by high-pressure NMR dynamics. *Nat. Catal.* **2**, 726–734. https://doi.org/10.1038/s41929-019-0307-6.
24. Bezsonova, I., Korzhnev, D.M., Prosser, R.S., Forman-Kay, J.D., Kay, L.E., (2006). Hydration and Packing along the Folding Pathway of SH3 Domains by Pressure-Dependent NMR. *Biochemistry* **45**, 4711–4719. https://doi.org/10.1021/bi060177r.
25. Tugarinov, V., Libich, D.S., Meyer, V., Roche, J., Clore, G. M., (2015). The Energetics of a Three-State Protein Folding System Probed by High-Pressure Relaxation Dispersion NMR Spectroscopy. *Angew. Chem. Int. Ed.* **54**, 11157–11161. https://doi.org/10.1002/anie.201505416.
26. Korzhnev, D.M., Bezsonova, I., Evanics, F., Taulier, N., Zhou, Z., Bai, Y., Chalikian, T.V., Prosser, R.S., et al., (2006). Probing the Transition State Ensemble of a Protein Folding Reaction by Pressure-Dependent NMR Relaxation Dispersion. *J. Am. Chem. Soc.* **128**, 5262–5269. https://doi.org/10.1021/ja0601540.
27. Xue, M., Wakamoto, T., Kejlberg, C., Yoshimura, Y., Nielsen, T.A., Risør, M.W., Sanggaard, K.W., Kitahara, R., et al., (2019). How internal cavities destabilize a protein. *PNAS* **116**, 21031–21036. https://doi.org/10.1073/pnas.1911181116.
28. Dreydoppel, M., Becker, P., Raum, H.N., Gröger, S., Balbach, J., Weininger, U., (2018). Equilibrium and Kinetic Unfolding of GB1: Stabilization of the Native State by Pressure. *J. Phys. Chem. B* **122**, 8846–8852. https://doi.org/10.1021/acs.jpcb.8b06888.
29. Dreydoppel, M., Dorn, B., Modig, K., Akke, M., Weininger, U., (2021). Transition-State Compressibility and Activation Volume of Transient Protein Conformational Fluctuations. *JACS Au.* **1**, 833–842. https://doi.org/10.1021/jacsau.1c00062.
30. Zhang, Y., Kitazawa, S., Peran, I., Stenzoski, N., McCallum, S.A., Raleigh, D.P., Royer, C.A., (2016). High Pressure ZZ-Exchange NMR Reveals Key Features of Protein Folding Transition States. *J. Am. Chem. Soc.* **138**, 15260–15266. https://doi.org/10.1021/jacs.6b09887.
31. Schütz, S., Sprangers, R., (2019). Methyl TROSY spectroscopy: A versatile NMR approach to study challenging biological systems. *Prog. Nucl. Magn. Reson. Spectrosc.*. https://doi.org/10.1016/j.pnmrs.2019.09.004. S0079656519300470.
32. Sprangers, R., Kay, L.E., (2007). Quantitative dynamics and binding studies of the 20S proteasome by NMR. *Nature* **445**, 618–622. https://doi.org/10.1038/nature05512.
33. Cvetkovic, M.A., Wurm, J.P., Audin, M.J., Schütz, S., Sprangers, R., (2017). The Rrp4-exosome complex recruits and channels substrate RNA by a unique mechanism. *Nat. Chem. Biol.* **13**, 522–528. https://doi.org/10.1038/nchembio.2328.
34. Rosenzweig, R., Moradi, S., Zarrine-Afsar, A., Glover, J.R., Kay, L.E., (2013). Unraveling the Mechanism of Protein Disaggregation Through a ClpB-DnaK Interaction. *Science* **339**, 1080–1083. https://doi.org/10.1126/science.1233066.
35. Jiang, Y., Kalodimos, C.G., (2017). NMR Studies of Large Proteins. *J. Mol. Biol.* **429**, 2667–2676. https://doi.org/10.1016/j.jmb.2017.07.007.
36. Audin, M.J.C., Dorn, G., Fromm, S.A., Reiss, K., Schütz, S., Vorländer, M.K., Sprangers, R., (2013). The archaeal exosome: identification and quantification of site-specific motions that correlate with cap and RNA binding. *Angew. Chem. Int. Ed. Engl.* **52**, 8312–8316. https://doi.org/10.1002/anie.201302811.
37. Tugarinov, V., Hwang, P.M., Ollerenshaw, J.E., Kay, L.E., (2003). Cross-Correlated Relaxation Enhanced $^{1}H-^{13}C$ NMR Spectroscopy of Methyl Groups in Very High Molecular Weight Proteins and Protein Complexes. *J. Am. Chem. Soc.* **125**, 10420–10428. https://doi.org/10.1021/ja030153x.
38. Wurm, J.P., Sprangers, R., (2019). Dcp2: an mRNA decapping enzyme that adopts many different shapes and forms. *Curr. Opin. Struct. Biol.* **59**, 115–123. https://doi.org/10.1016/j.sbi.2019.07.009.
39. Wurm, J.P., Holdermann, I., Overbeck, J.H., Mayer, P.H. O., Sprangers, R., (2017). Changes in conformational equilibria regulate the activity of the Dcp2 decapping enzyme. *Proc. Natl. Acad. Sci.* **114**, 6034–6039. https://doi.org/10.1073/pnas.1704496114.
40. Floor, S.N., Borja, M.S., Gross, J.D., (2012). Interdomain dynamics and coactivation of the mRNA decapping enzyme Dcp2 are mediated by a gatekeeper tryptophan. *PNAS* **109**, 2872–2877. https://doi.org/10.1073/pnas.1113620109.
41. Charenton, C., Taverniti, V., Gaudon-Plesse, C., Back, R., Séraphin, B., Graille, M., (2016). Structure of the active form of Dcp1–Dcp2 decapping enzyme bound to m7GDP and its Edc3 activator. *Nat. Struct. Mol. Biol.* **23**, 982–986. https://doi.org/10.1038/nsmb.3300.
42. Wurm, J.P., Overbeck, J., Sprangers, R., (2016). The S. Pombe mRNA decapping complex recruits cofactors and an Edc1-like activator through a single dynamic surface. *RNA* **22**, 1360–1372. https://doi.org/10.1261/rna.057315.116.
43. She, M., Decker, C.J., Svergun, D.I., Round, A., Chen, N., Muhlrad, D., Parker, R., Song, H., (2008). Structural Basis of Dcp2 Recognition and Activation by Dcp1. *Mol. Cell* **29**, 337–349. https://doi.org/10.1016/j.molcel.2008.01.002.
44. Mugridge, J.S., Ziemniak, M., Jemielity, J., Gross, J.D., (2016). Structural basis of mRNA-cap recognition by Dcp1–Dcp2. *Nat. Struct. Mol. Biol.* **23**, 987–994. https://doi.org/10.1038/nsmb.3301.
45. Goto, N.K., Kay, L.E., (2000). New developments in isotope labeling strategies for protein solution NMR spectroscopy. *Curr. Opin. Struct. Biol.* **10**, 585–592. https://doi.org/10.1016/S0959-440X(00)00135-4.
46. Kerfah, R., Plevin, M.J., Sounier, R., Gans, P., Boisbouvier, J., (2015). Methyl-specific isotopic labeling: a molecular tool box for solution NMR studies of large proteins. *Curr. Opin. Struct. Biol.* **32**, 113–122. https://doi.org/10.1016/j.sbi.2015.03.009.
47. Chen, C.R., Makhatadze, G.I., (2015). ProteinVolume: calculating molecular van der Waals and void volumes in

proteins. *BMC Bioinf.* **16**, 101. https://doi.org/10.1186/s12859-015-0531-2.
48. Beck Erlach, M., Koehler, J., Crusca, E., Munte, C.E., Kainosho, M., Kremer, W., Kalbitzer, H.R., (2017). Pressure dependence of side chain 13C chemical shifts in model peptides Ac-Gly-Gly-Xxx-Ala-NH2. *J. Biomol. NMR* **69**, 53–67. https://doi.org/10.1007/s10858-017-0134-5.
49. Akasaka, K., Li, H., Yamada, H., Li, R., Thoresen, T., Woodward, C.K., (1999). Pressure response of protein backbone structure. Pressure-induced amide $^{15}$N chemical shifts in BPTI. *Protein Sci.* **8**, 1946–1953. https://doi.org/10.1110/ps.8.10.1946.
50. Akasaka, K., Li, H., (2001). Low-Lying Excited States of Proteins Revealed from Nonlinear Pressure Shifts in $^{1}$ H and $^{15}$ N NMR. *Biochemistry* **40**, 8665–8671. https://doi.org/10.1021/bi010312u.
51. Gagné, D., Azad, R., Edupuganti, U.R., Williams, J., Aramini, J.M., Akasaka, K., Gardner, K.H., (2020). Use of High Pressure NMR Spectroscopy to Rapidly Identify Proteins with Internal Ligand-Binding Voids. *BioRxiv 2020.08.25.267195*. https://doi.org/10.1101/2020.08.25.267195.
52. Maeno, A., Sindhikara, D., Hirata, F., Otten, R., Dahlquist, F.W., Yokoyama, S., Akasaka, K., Mulder, F.A.A., et al., (2015). Cavity as a Source of Conformational Fluctuation and High-Energy State: High-Pressure NMR Study of a Cavity-Enlarged Mutant of T4Lysozyme. *Biophys. J.* **108**, 133–145. https://doi.org/10.1016/j.bpj.2014.11.012.
53. Alderson, T.R., Kay, L.E., (2020). Unveiling invisible protein states with NMR spectroscopy. *Curr. Opin. Struct. Biol.* **60**, 39–49. https://doi.org/10.1016/j.sbi.2019.10.008.
54. Baldwin, A.J., Kay, L.E., (2009). NMR spectroscopy brings invisible protein states into focus. *Nat. Chem. Biol.* **5**, 808–814. https://doi.org/10.1038/nchembio.238.
55. Bouvignies, G., Vallurupalli, P., Hansen, D.F., Correia, B. E., Lange, O., Bah, A., Vernon, R.M., Dahlquist, F.W., et al., (2011). Solution structure of a minor and transiently formed state of a T4 lysozyme mutant. *Nature* **477**, 111–114. https://doi.org/10.1038/nature10349.
56. Delaglio, F., Grzesiek, S., Vuister, G.W., Zhu, G., Pfeifer, J., Bax, A., (1995). NMRPipe: a multidimensional spectral processing system based on UNIX pipes. *J. Biomol. NMR* **6**, 277–293.
57. Lundström, P., Vallurupalli, P., Religa, T.L., Dahlquist, F. W., Kay, L.E., (2007). A single-quantum methyl 13C-relaxation dispersion experiment with improved sensitivity. *J. Biomol. NMR* **38**, 79–88. https://doi.org/10.1007/s10858-007-9149-7.
58. Baldwin, A.J., (2014). An exact solution for R2, eff in CPMG experiments in the case of two site chemical exchange. *J. Magn. Reson.* **244**, 114–124. https://doi.org/10.1016/j.jmr.2014.02.023.
59. Ho, B.K., Gruswitz, F., (2008). HOLLOW: Generating Accurate Representations of Channel and Interior Surfaces in Molecular Structures. *BMC Struct. Biol.* **8**, 49. https://doi.org/10.1186/1472-6807-8-49.
60. Pettersen, E.F., Goddard, T.D., Huang, C.C., Couch, G.S., Greenblatt, D.M., Meng, E.C., Ferrin, T.E., (2004). UCSF Chimera? A visualization system for exploratory research and analysis. *J. Comput. Chem.* **25**, 1605–1612. https://doi.org/10.1002/jcc.20084.